567819

NASA Contractor Report 185189

Finite Element Analysis of Structural Components Using Viscoplastic Models With Application to a Cowl Lip Problem

V.K. Arya

University of Toledo
Toledo, Ohio

June 1990

ORIGINAL CONTAINS
COLOR ILLUSTRATIONS

NASA
National Aeronautics and
Space Administration

FINITE ELEMENT ANALYSIS OF STRUCTURAL COMPONENTS USING VISCOPLASTIC

MODELS WITH APPLICATION TO A COWL LIP PROBLEM

V.K. Arya*
Department of Mechanical Engineering
University of Toledo
Toledo, Ohio 43606

ABSTRACT

The viability of advanced viscoplastic models for nonlinear finite element analyses of structural components is investigated. Several uniaxial and a multiaxial problem are analyzed using the finite element implementation of Freed's viscoplastic model. Good agreement between the experimental and calculated uniaxial results validates the finite element implementation and gives confidence to apply it to more complex multiaxial problems. A comparison of results for a sample structural component (the cowl lip of a hypersonic engine inlet) with the earlier elastic, elastic-plastic, and elastic-plastic-creep analyses available in the literature shows that the elastic-viscoplastic analyses yield more reasonable stress and strain distributions. Finally, the versatility of the finite-element-based solution technology presented herein is demonstrated by applying it to another viscoplastic model.

INTRODUCTION

During the last two decades, a number of stress-strain constitutive models (called viscoplastic models) have emerged. The motivation in the development of these models has been to incorporate observed high-temperature plasticity and creep interactions. This is achieved by treating all the inelastic strain (plastic, creep, relaxation, etc.) as a single unified quantity, and thus automatically including any interactions among them.

―――――――――

*NASA Resident Research Associate at Lewis Research Center.

Viscoplastic models are intended to provide more realistic descriptions of high-temperature, time-dependent, inelastic behavior of materials. The attempt to make these models realistic by including as much material science as possible renders their mathematical framework complicated. The differential equations defining the flow and evolutionary laws of the models are, in general, highly nonlinear and mathematically stiff. High-temperature structural components (such as those used in aerospace or nuclear industries) involve complex geometries as well as thermal and mechanical loadings. Closed-form analytical solutions for these problems are intractable. Thus, in order to use viscoplastic models in nonlinear structural analyses for component design, it becomes mandatory to develop and verify suitable numerical solution technologies involving, for instance, the finite element method.

With these requirements in mind, the advantages of employing realistic viscoplastic models for nonlinear finite element analyses of structural components are explored by analyzing several uniaxial problems and a multiaxial problem. The viscoplastic model developed by Freed[1], and characterized for copper, was employed to describe the time-dependent inelastic behavior of the material. This viscoplastic model, in its general multiaxial form, was implemented in the finite element program MARC[2]. The implementation was exercised first on several uniaxial problems involving isothermal and nonisothermal cyclic loadings. The results thus obtained were compared with the experimental results from Reference 1. This was done to validate the finite element implementation. The validated implementation was then applied for stress analysis of a sample structural component. The component, called a cowl lip, is part of the leading edge of a hypersonic aircraft engine inlet and is subjected to severe thermal loading and gradients. Finally, the versatility of the finite-element-based solution technology developed for Freed's model was determined by using it for another viscoplastic model developed by Robinson[3].

2

For completeness, a brief description of Freed's viscoplastic model is provided in the following section.

FREED'S VISCOPLASTIC MODEL

Following the general mathematical structure adopted by the majority of viscoplastic models, Freed's model also incorporates two internal state variables, namely, a back stress and a drag strength. The tensorial valued back stress accounts for strain-induced or kinematic hardening, whereas isotropic hardening in the model is introduced via scalar valued drag strength. A small strain and a small displacement formulation are employed. It is assumed that there is no explicit coupling between the static and dynamic recovery terms in an evolutionary equation for the internal state. This imparts a simpler mathematical framework for the model.

The total strain rate $\dot{\varepsilon}_{ij}$ is written as the sum of elastic $\dot{\varepsilon}_{ij}^{el}$, inelastic (including plasticity, creep, relaxation, etc.) $\dot{\varepsilon}_{ij}^{in}$, and thermal $\dot{\varepsilon}_{ij}^{th}$, rate components. In symbols

$$\dot{\varepsilon}_{ij} = \dot{\varepsilon}_{ij}^{el} + \dot{\varepsilon}_{ij}^{in} + \dot{\varepsilon}_{ij}^{th} \qquad (i,j = 1,2,3) \tag{1}$$

Here ε denotes the strain, and a dot over a symbol indicates its derivative with respect to time t.

The material is assumed to be isotropic, and Hooke's law is used to relate the elastic strain rate $\dot{\varepsilon}_{ij}^{el}$ to the stress rate $\dot{\sigma}_{ij}$; that is,

$$\dot{\varepsilon}_{ij}^{el} = \frac{1 + \nu}{E} \dot{\sigma}_{ij} - \frac{\nu}{E} \dot{\sigma}_{kk} \delta_{ij} \tag{2}$$

where E is Young's modulus, ν is Poisson's ratio, and δ_{ij} is the Kronecker delta. Following Einstein's summation convention, the repeated subscripts in equation (2) and elsewhere imply summation.

The deviatoric stress S_{ij} has the expression

$$S_{ij} = \sigma_{ij} - \frac{1}{3} \sigma_{kk} \delta_{ij} \tag{3}$$

With the back stress denoted by B_{ij}, the effective stress Σ_{ij} is defined as

$$\Sigma_{ij} = S_{ij} - B_{ij} \tag{4}$$

The constitutive equations of the model are:

Flow Law

$$\dot{\varepsilon}_{ij}^{in} = \Theta Z \frac{\Sigma_{ij}}{J_2} \tag{5}$$

where

$$J_2 = \frac{1}{2} \Sigma_{ij}\Sigma_{ij} \tag{6}$$

The temperature dependence of the model is mainly contained in the thermal-diffusivity, function Θ, which is defined as

$$\Theta = \begin{cases} \exp\left(-\dfrac{Q}{kT}\right) \; ; & T \geq 0.5\, T_m \\[2mm] \exp\left\{-\dfrac{2Q}{kT_m}\left[\ln\left(\dfrac{T_m}{2T}\right) + 1\right]\right\} \; ; & T \leq 0.5\, T_m \end{cases} \tag{7}$$

in which equation Q is the activation energy, k is the Boltzmann constant, T is the absolute temperature, and T_m is the melting point of the material.

The function Z, called the Zener-Hollomon parameter, has the following expressions:

$$Z = \begin{cases} AF^n \; ; & F \leq 1 \\[1mm] A\, \exp[n(F - 1)] \; ; & F \geq 1 \end{cases} \tag{8}$$

where A and n are material constants. The function F is defined as

$$F = \frac{J_2}{D} \tag{9}$$

Here D denotes the drag strength.

Evolutionary Laws

The differential equations governing the growth of the internal state variables (i.e., the back stress B_{ij} and the drag strength D) are

$$\dot{B}_{ij} = H\left(\dot{\varepsilon}_{ij}^{in} - \frac{B_{ij}}{L} I_2\right) \tag{10}$$

and

$$\dot{D} = h\left[\frac{I_2}{G} - \Theta r(G)\right] \tag{11}$$

where

$$I_2 = \Theta Z$$

In equations (10) and (11), H, h, and L are inelastic material constants. The constant L denotes the limiting value of the back stress at kinematic saturation[1]. The recovery function r is defined through the following equations:

$$r(G) = \begin{cases} 0 \ ; & D = D_0 \\ R(G) \ ; & D > D_0 \end{cases} \tag{12}$$

$$R(G) = \begin{cases} AG^{n-1} \ ; & G \leq 1 \\ A \exp[n(G - 1)]/G \ ; & G \geq 1 \end{cases} \tag{13}$$

and

$$G = \frac{L}{S - D} \tag{14}$$

where S and D_0 are material constants.

Further, satisfying the dissipativity condition results in the following constraint on the function r

$$r \geq Z\left[\frac{1}{G} - 2\left(F + \frac{B_2^2}{LD}\right)\right] \tag{15}$$

5

where

$$B_2 = \frac{1}{2} B_{ij} B_{ij} \qquad (16)$$

This condition must be satisfied for the theory to be thermodynamically admissible.

The highly nonlinear and mathematically stiff nature of the constitutive equations requires the development of suitable numerical solution technologies (involving, for example, the finite element method) to facilitate the application of these models in component design. A brief description of the finite-element-based solution technology is provided hereunder.

FINITE ELEMENT SOLUTIONS

The finite element solutions using Freed's model for both the uniaxial and multiaxial cowl lip problem were obtained by using the general purpose finite element program MARC. The MARC program was developed expressly for nonlinear structural analyses and is well equipped with sophisticated computational algorithms and advanced finite element formulations.

The viscoplastic model of Freed was implemented in MARC through the user subroutine HYPELA. The implementation of Freed's model follows essentially the same methodology that was utilized earlier by Arya and Kaufman[4] for Robinson's model.

The mathematically stiff nature of the constitutive equations poses significant difficulty in their time integration. Smart time-integration strategies are required to integrate these equations efficiently and accurately. In the present work, a self-adaptive time integration strategy developed by Arya et al.[5] was utilized. The strategy is based on the explicit Forward Euler method. An explicit method does not require the assembly or inversion of Jacobian matrices and thus is more pertinent for problems with

6

large degrees of freedom. The integration strategy used here has been applied to other problems in Reference 6, where it was found to work successfully.

STRESS ANALYSES

Several uniaxial problems and a multiaxial cowl lip problem were analyzed with this finite element implementation.

The uniaxial loadings shown in Figure 1 consist of mechanical and thermal (both isothermal and nonisothermal) loadings. The nonisothermal loadings included in-phase and out-of-phase loadings. The material constants characterizing copper, taken from Reference 1, are listed in Table 1.

For the stress analysis of the multiaxial cowl lip problem, a finite element model constructed by Melis and Gladden[7] was utilized. This model, shown in Figure 2, is made up of 3294 solid eight-noded brick elements and has 4760 nodes. The dimensions of the cowl lip are approximately 6 by 1.5 by 0.25 in. (15.2 by 3.8 by 0.64 cm). However, for the finite element analysis, only the 2-in. (5-cm) central portion of the component was modeled to avoid difficult-to-quantify end effects. A large number of elements were required to handle the severity of the thermal loading and gradients. The severity of thermal loading, illustrated in Figure 3, can be judged by noticing that the temperature at a critical location of the cowl lip rises from 21 to 758 °C in only 0.75 sec (Figure 4). However, by taking advantage of the symmetry along the thickness, only half of the model was utilized in numerical computations. This resulted in a considerable saving in CPU time.

RESULTS AND DISCUSSION

Uniaxial Problems

Predicted hysteresis loops for isothermal and nonisothermal (both in-phase and out-of-phase) loadings are shown in Figure 1 and plotted in Figures 5 to 7. The strain range for the isothermal loops is 2 percent and the strain rate is 0.001/sec. The strain range for nonisothermal loops is 0.8 percent and the

strain rate is 1.5×10^{-5}/sec. To facilitate comparison, the experimental hysteresis loops are also plotted in these figures.

Figure 5 exhibits the calculated and experimental hysteresis loops for isothermal loadings at temperatures of 22 and 600 °C. A comparison of these figures reveals good agreement between the experimental and correlated stabilized hysteresis loops obtained with the finite element implementation.

The predicted and experimental hysteresis loops for the in-phase and out-of-phase loadings are depicted in Figures 6 and 7, respectively. The strain range for these loops is 0.8 percent and the strain rate is 1.5×10^{-5}/sec. By comparing these figures, it is found that the calculated loops overpredict the stress actually seen in the experiments, especially at the cold end of the cycle. In general, however, the agreement between the experimental and predicted loops is good. This overprediction of stress at the cold ends is inherent in the model, and is also seen in the results of Reference 1.

Multiaxial Cowl Lip Problem

The steady-state temperature distribution in the cowl lip, obtained from Melis and Gladden[7], is depicted in Figure 7. The highest temperatures are found to occur along the leading edge. A linear interpolation technique was employed to estimate the transient temperature distribution in the cowl lip. The temperature values thus obtained were used to perform time-dependent inelastic stress analyses.

To assess the advantages offered by more realistic elastic-viscoplastic analysis, it is appropriate to reproduce some earlier results from elastic, elastic-plastic, and elastic-plastic-creep analyses of the cowl lip. These results, taken from Arya et al.[8], are shown in Figures 8 to 10. A primary creep law was used by Arya et al. for the elastic-plastic-creep analysis. Figures 8 to 10 exhibit the various stress distributions during steady-state thermal loading across a cross section of the component.

Figure 8 presents the elastic stress distribution in the cowl lip. The stress values (in magnitude) are seen to be well above the yield strength of the copper cowl lip material and are thus unrealistic. The high temperatures and thermal gradients along the edge of the cowl lip are expected to cause significant inelastic deformation. This consideration led Arya et al.[8] to perform elastic-plastic and elastic-plastic-creep analyses for the component. The results of these analyses are depicted in Figures 9 and 10, which exhibit the stress along the edge of the cowl lip. The magnitude of the largest stress for both of these analyses is observed to be reduced appreciably from that obtained by purely elastic analysis.

The results of the current elastic-viscoplastic analysis using Freed's model are shown in Figures 11 to 13. Figure 11 exhibits the stress distribution along the edge at 0.75 sec. The total strain in Figure 12 is the sum of elastic, inelastic, and thermal strains. Figure 13 displays the stress at 2.25 sec. A comparison of Figures 8 to 11 reveals that the magnitude of maximum stress drops continuously from elastic to elastic-plastic to elastic-viscoplastic analyses. In Figure 12 the largest total strain is observed to occur along the edge of the cowl lip. It is interesting to note that the elastic-viscoplastic model is capable of capturing the redistribution of stress even during a small period of steady-state thermal loading between 0.75 and 2.25 sec. This redistribution of stress is apparent on comparing Figure 11 with Figure 13. The elastic-plastic-creep analysis of Reference 8 was unable to depict this redistribution of stress with time.

ADAPTABILITY OF SOLUTION TECHNOLOGY FOR OTHER VISCOPLASTIC MODELS

The versatility of the finite-element-based solution technology developed during the present work for other viscoplastic models was also investigated. It is very encouraging to note that the solution technology easily adapts itself for use with other models. As an example, the cowl lip problem was also

analyzed by using Robinson's model[3]. The material constants used in these computations are for a copper alloy, Narloy-Z[9].

Some results of this analysis are shown in Figures 14 to 16. Figures 14 and 15 depict the stress and total strain distributions along the edge of the cowl lip at 0.75 sec. The stress along the edge at 2.25 sec is exhibited in Figure 16. These figures exhibit trends similar to those observed with Freed's model for copper. From Figures 14 and 15, the largest stress and total strain are found to occur along the edge of the cowl lip. A comparison of Figure 14 with Figure 16 clearly shows the capability of this viscoplastic model to also predict the redistribution of stress during the steady thermal loading from 0.75 to 2.25 sec.

CONCLUSIONS

A numerical solution technology employing the finite element method was developed to perform the nonlinear structural analyses using viscoplastic models. The technology is illustrated for Freed's model but is general in nature. Several uniaxial problems, as well as a multiaxial cowl lip problem, were analyzed. Good agreement between the experimental and predicted hysteresis loops for uniaxial thermomechanical loadings confirms the correct finite element implementation of the viscoplastic model. By using this validated implementation, a finite element analysis is performed for the multiaxial cowl lip problem. The advantages of employing realistic viscoplastic models are apparent on comparing the results thus obtained with the elastic, elastic-plastic, and elastic-plastic-creep analyses. The versatility of the finite-element-based solution technology developed herein is demonstrated by applying it successfully to another viscoplastic model, specifically, that of Robinson.

REFERENCES

1 Freed, A.D. and Verrilli, M.J. A viscoplastic theory applied to copper, <u>NASA TM-100831</u> (1988)

2 <u>MARC General Purpose Finite Element Program</u>, MARC Research Analysis Research Corp., Palo Alto, CA (1983)

3 Robinson, D.N. and Swindeman, R.W. Unified creep-plasticity constitutive equations for 2-1/4 Cr-1 Mo steel at elevated temperature, <u>ORNL/TM-8444</u> (1982)

4 Arya, V.K. and Kaufman, A. Finite element implementation of Robinson's viscoplastic model and its application to some uniaxial and multiaxial problems, <u>Engineering Computations</u>, 6, 3, pp. 537-547 (1989)

5 Arya, V.K., Hornberger, K., and Stamm, H. On the numerical integration of viscoplastic models, <u>KfK-4082</u> (1986)

6 Arya, V.K. Analytical and finite element solutions of some problems using a viscoplastic model, <u>Journal of Computers and Structures</u>, 33, 4, pp. 957-967 (1989)

7 Melis, M.E. and Gladden, H.J. Thermostructural analysis with experimental verification in a high heat flux facility of a simulated cowl lip, <u>29th Structures, Structural Dynamics and Materials Conference</u>, Part 1, AIAA, New York, pp. 106-115 (1988)

8 Arya, V.K., Melis, M.E., and Halford, G.R. A finite element elastic-plastic-creep and cyclic life analysis of a cowl lip, <u>NASA TM-102342</u> (1989)

9 Robinson, D.N. and Arnold, S.M. Effects of state recovery on creep buckling under variable loading, <u>NASA CR-175094</u> (1985)

11

Table 1 Material constants for copper

A, s^{-1}	50 000 000
D_O, MPa	1.5
E, MPa	165 000 – 125 T
H, MPa	5000
h, MPa	500
L, MPa	25 exp($-T/300$)
n	5
Q, J/mol	200 000
S, MPa	14.3
T_m, K	1356
α, °C^{-1} . . .	15x10^{-6} + 5x10^{-9} T
ν	0.34

Notes:
1. 1 MPa = 0.145 ksi
2. Temperature T in degrees
   Celsius
   [°C = (°F – 32)/1.8)]
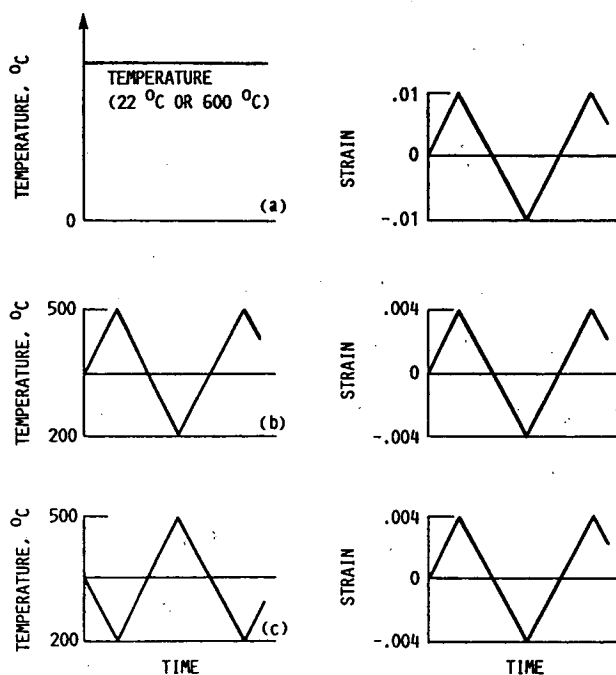
(a) Isothermal loading.
(b) Nonisothermal (in-phase) loadings.
(c) Nonisothermal (out-of-phase) loadings.

Figure 1.—Cyclic thermal and mechanical loading used to generate hysteresis loops by the MARC finite element code.
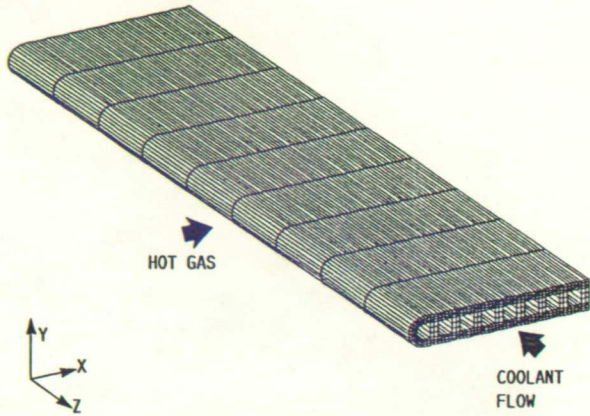
Figure 2.—Cowl lip finite element model. Elements, 3294; nodes, 4760.
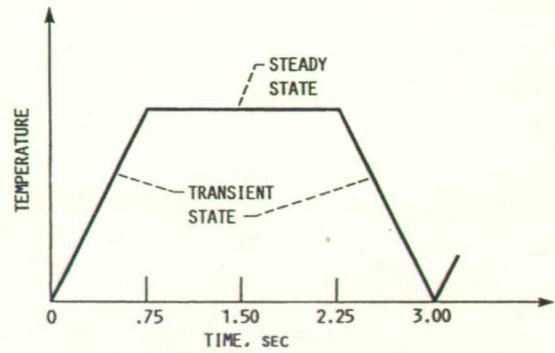
Figure 3.—Thermal loading cycle for cowl lip problem.
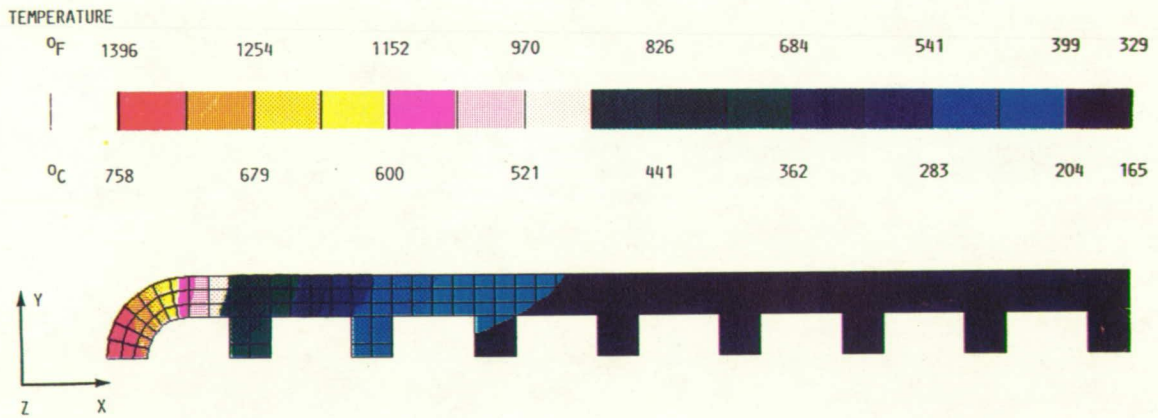
Figure 4.—Steady-state temperature distribution in copper cowl lip. Time, 0.75 to 2.25 sec; cross flow, GH_2 coolant.
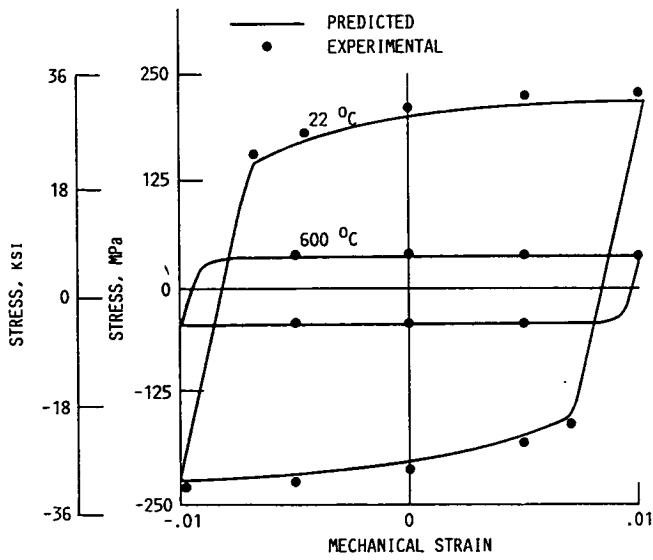
13

Figure 5.—Predicted stabilized hysteresis loops for copper using Freed's model (isothermal loading). Experimental data from Freed and Verrilli (ref. 1). Strain rate, 0.001/sec.
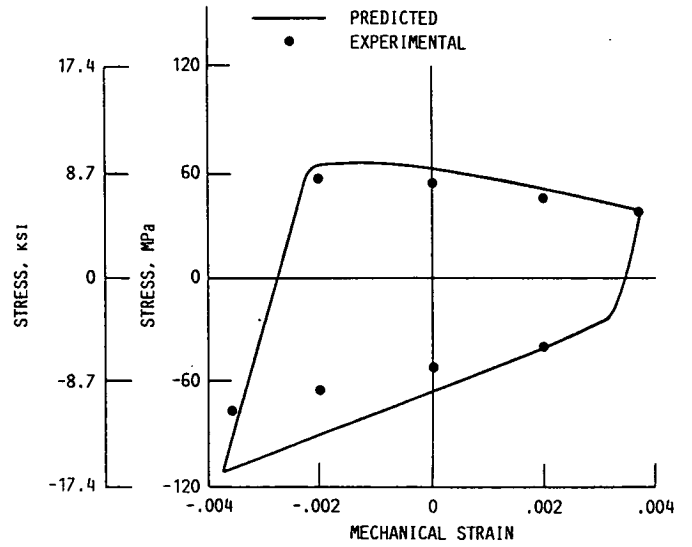

Figure 6.—In-phase predicted hysteresis loops for copper using Freed's model. Experimental data from Freed and Verrilli (ref.1). Temperature, 200 ⇌ 500 °C; strain rate, 1.5x10^{-5}/sec.
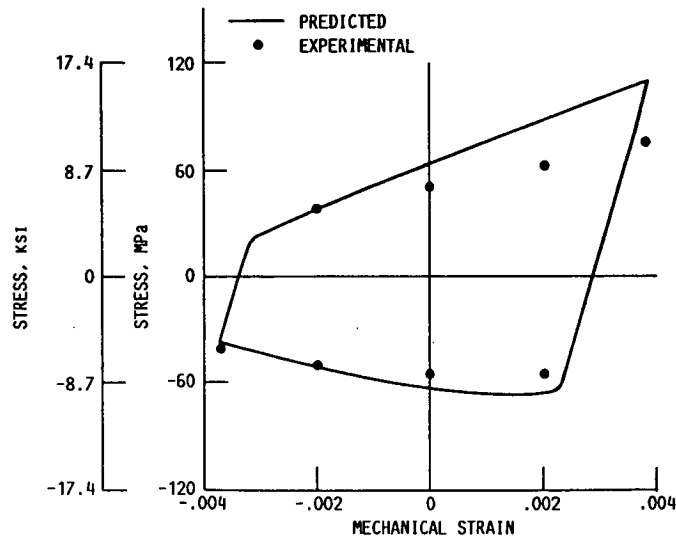
Figure 7.—Out-of-phase predicted hysteresis loops for copper using Freed's model. Experimental data from Freed and Verrilli (ref.1). Temperature, 200 ⇌ 500 °C; strain rate, 2.5x10^{-5}/sec.
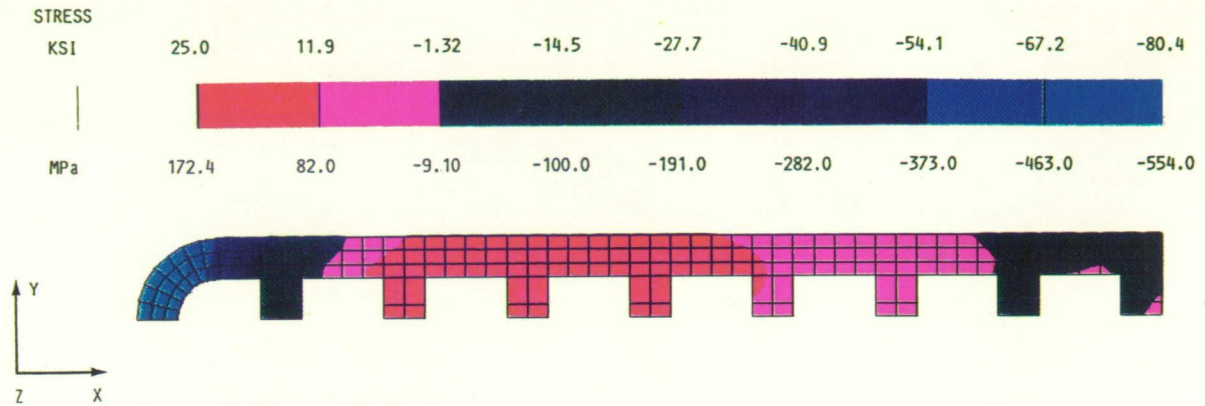
STRESS

KSI	25.0	11.9	-1.32	-14.5	-27.7	-40.9	-54.1	-67.2	-80.4
MPa	172.4	82.0	-9.10	-100.0	-191.0	-282.0	-373.0	-463.0	-554.0

Figure 8.—Stress in Z-direction in copper cowl lip; elastic analysis. Cross flow, GH$_2$ coolant.

STRESS

KSI	12.1	6.27	.476	-5.32	-11.1	-16.9	-22.7	-28.5
MPa	83.4	43.2	3.3	-36.7	-76.5	-116.5	-156.5	-196.5
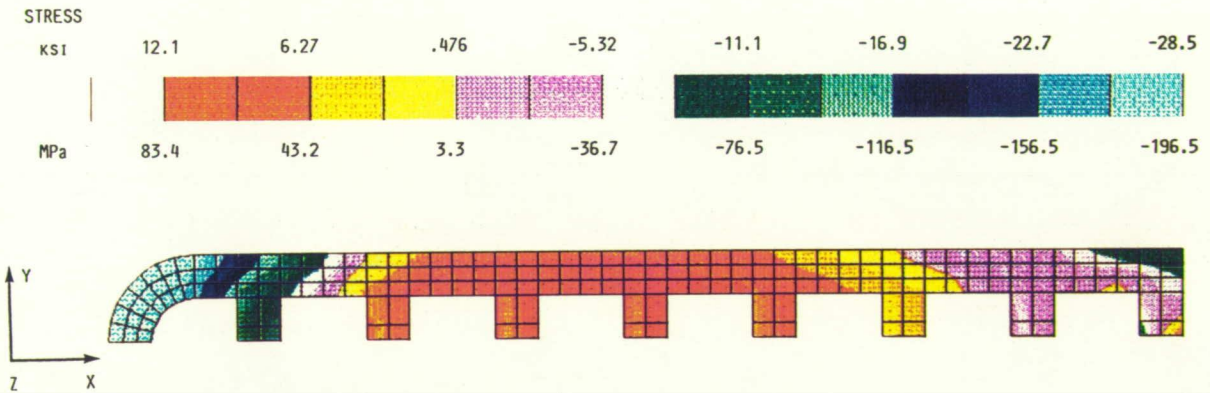
Figure 9.—Stress in Z-direction in copper cowl lip; elastic-plastic analysis. Cross flow, GH$_2$ coolant.

STRESS

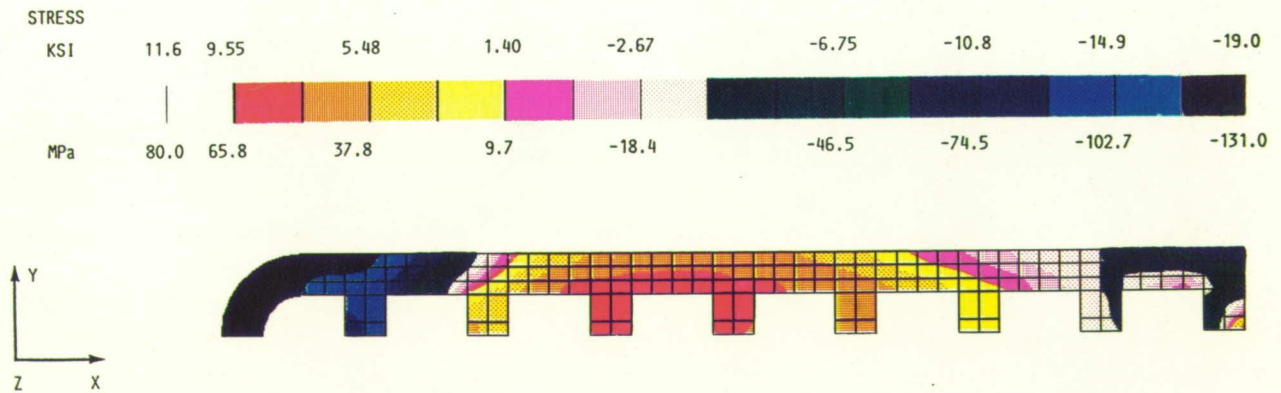| KSI	11.6	9.55	5.48	1.40	-2.67	-6.75	-10.8	-14.9	-19.0
MPa	80.0	65.8	37.8	9.7	-18.4	-46.5	-74.5	-102.7	-131.0

Figure 10.—Stress in Z-direction in copper cowl lip; elastic-plastic-creep analysis. Time, 0.75 sec; cross flow, GH$_2$ coolant.
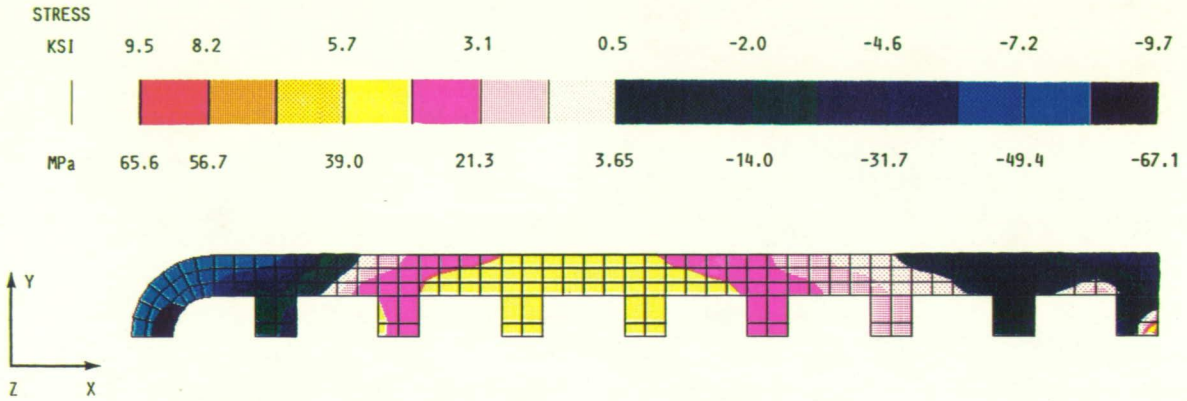
17

Figure 11.—Stress in Z-direction in copper cowl lip; elastic-viscoplastic analysis (Freed's model). Time, 0.75 sec; cross flow, GH$_2$ coolant.
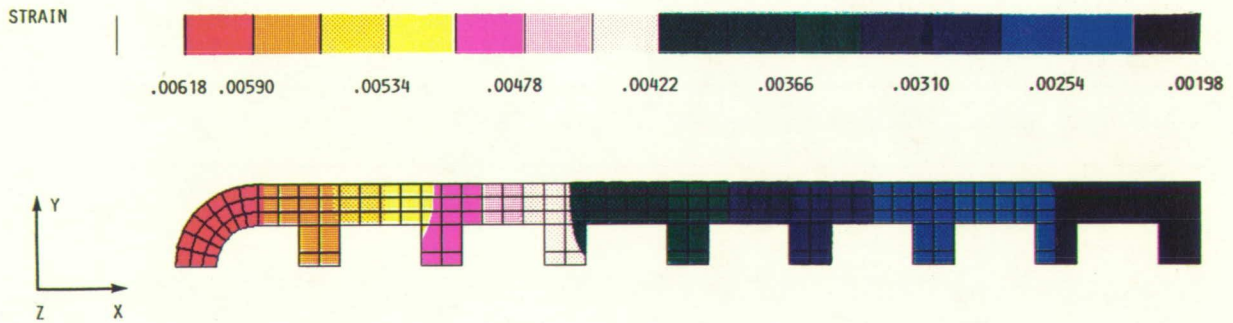

Figure 12.—Total strain in Z-direction in copper cowl lip; elastic-viscoplastic analysis (Freed's model). Time, 0.75 sec; cross flow, GH$_2$ coolant.
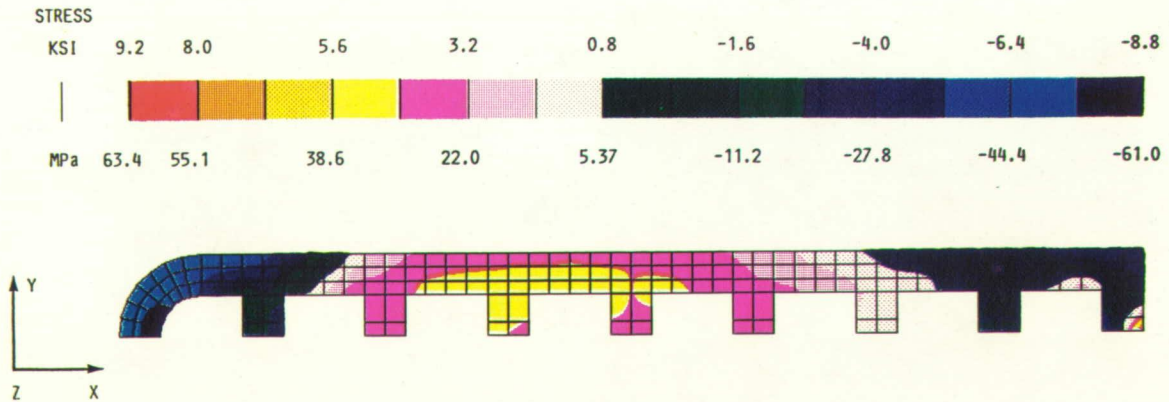

Figure 13.—Stress in Z-direction in copper cowl lip; elastic-viscoplastic analysis (Freed's model). Time, 2.25 sec; cross flow, GH$_2$ coolant.
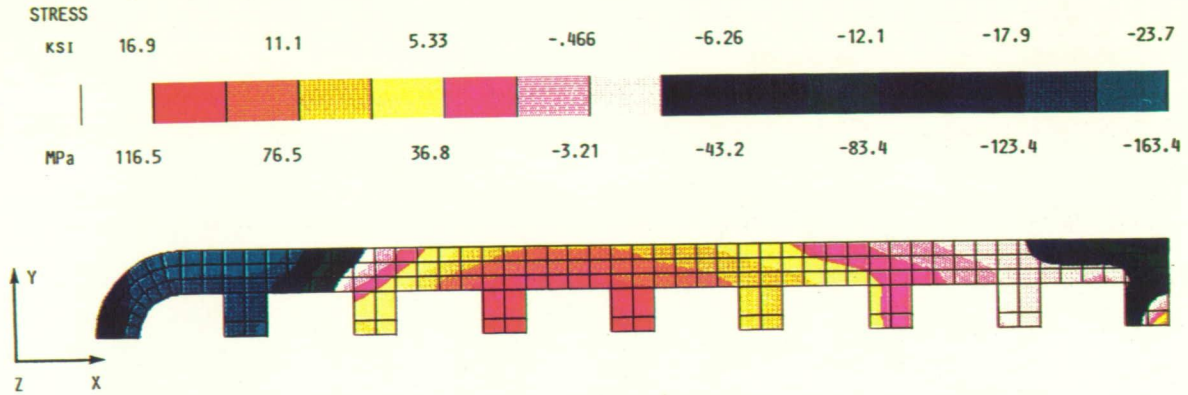
19

Figure 14.—Stress in Z-direction in copper alloy Narloy-Z cowl lip; elastic-viscoplastic analysis (Robinson's model). Time, 0.75 sec; cross flow, GH_2 coolant.
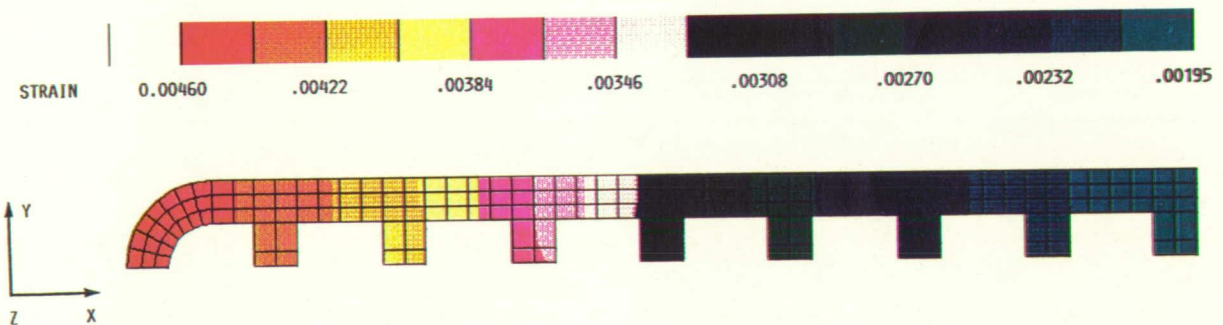

Figure 15.—Total strain in Z-direction in copper alloy Narloy-Z cowl lip; elastic-viscoplastic analysis (Robinson's model). Time, 0.75 sec; cross flow, GH_2 coolant.
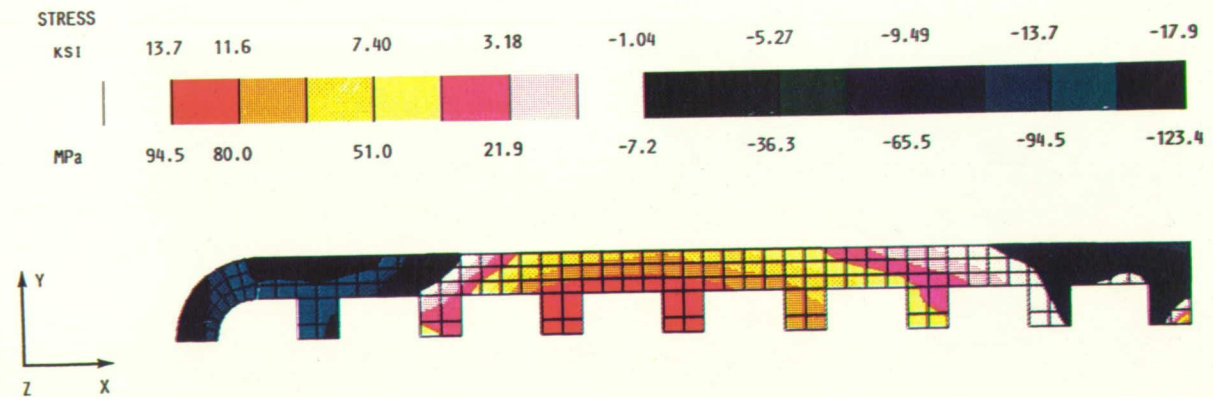

Figure 16.—Stress in Z-direction in copper alloy Narloy-Z cowl lip; elastic-viscoplastic analysis (Robinson's model). Time, 2.25 sec; cross flow, GH_2 coolant.

21

NASA
National Aeronautics and Space Administration

Report Documentation Page

1. Report No.	2. Government Accession No.	3. Recipient's Catalog No.
NASA CR-185189		

4. Title and Subtitle		5. Report Date
Finite Element Analysis of Structural Components Using Viscoplastic Models With Application to a Cowl Lip Problem		June 1990
		6. Performing Organization Code

7. Author(s)		8. Performing Organization Report No.
V.K. Arya		None (E-4920)
		10. Work Unit No.
		510-01-01

9. Performing Organization Name and Address	11. Contract or Grant No.
University of Toledo Toledo, Ohio 43606	NCC3-120
	13. Type of Report and Period Covered

12. Sponsoring Agency Name and Address	Contractor Report Final
National Aeronautics and Space Administration Lewis Research Center Cleveland, Ohio 44135-3191	14. Sponsoring Agency Code

15. Supplementary Notes

16. Abstract

The viability of advanced viscoplastic models for nonlinear finite element analyses of structural components is investigated. Several uniaxial and a multiaxial problem are analyzed using the finite element implementation of Freed's viscoplastic model. Good agreement between the experimental and calculated uniaxial results validates the finite element implementation and gives confidence to apply it to more complex multiaxial problems. A comparison of results for a sample structural component (the cowl lip of a hypersonic engine inlet) with the earlier elastic, elastic-plastic, and elastic-plastic-creep analyses available in the literature shows that the elastic-viscoplastic analyses yield more reasonable stress and strain distributions. Finally, the versatility of the finite-element-based solution technology presented herein is demonstrated by applying it to another viscoplastic model.

17. Key Words (Suggested by Author(s))	18. Distribution Statement
Nonlinear structural analysis; Viscoplasticity; Cowl lip; Finite element analysis	Unclassified – Unlimited Subject Category 39

19. Security Classif. (of this report)	20. Security Classif. (of this page)	21. No. of pages	22. Price*
Unclassified	Unclassified	22	A03

NASA FORM 1626 OCT 86   *For sale by the National Technical Information Service, Springfield, Virginia 22161

National Aeronautics and
Space Administration

Lewis Research Center
Cleveland, Ohio 44135

FOURTH CLASS MAIL

ADDRESS CORRECTION REQUESTED

NASA